The Goos-Hänchen effect for surface plasmon polaritons

Felix Huerkamp,[1,2,*] **Tamara A. Leskova,**[1,4] **Alexei A. Maradudin,**[1] **and Björn Baumeier**[3]

[1] *Department of Physics and Astronomy and Institute for Surface and Interface Science, University of California, Irvine CA 92697, USA*
[2] *Westfälische Wilhelms-Universität Münster, Wilhelm-Klemm-Str. 10, 48149 Münster, Germany*
[3] *Max Planck Institute for Polymer Research, Ackermannweg 10, 55128 Mainz, Germany*
[4] *deceased*
[*] *felix.huerkamp@uni-muenster.de*

Abstract: By means of an impedance boundary condition and numerical solution of integral equations for the scattering amplitudes to which its use gives rise, we study as a function of its angle of incidence the reflection of a surface plasmon polariton beam propagating on a metal surface whose dielectric function is $\varepsilon_1(\omega)$ when it is incident on a planar interface with a coplanar metal surface whose dielectric function is $\varepsilon_2(\omega)$. When the surface of incidence is optically more dense than the surface of scattering, i.e. when $|\varepsilon_2(\omega)| \gg |\varepsilon_1(\omega)|$, the reflected beam undergoes a lateral displacement whose magnitude is several times the wavelength of the incident beam. This displacement is the surface plasmon polariton analogue of the Goos-Hänchen effect. Since this displacement is sensitive to the dielectric properties of the surface, this effect can be exploited to sense modifications of the dielectric environment of a metal surface, e.g. due to adsorption of atomic or molecular layers on it.

OCIS codes: (240.6680) Surface plasmons; (240.5420) Polaritons; (290.5825) Scattering theory

References and links

1. F. Goos and H. Hänchen, "Ein neuer und fundamentaler Versuch zur Totalreflexion," Ann. Phys. **436**, 333–346 (1947).
2. K. Artmann, "Berechnung der Seitenversetzung des totalreflektierten Strahles," Ann. Phys. **437**, 87–102 (1948).
3. H. Shin and S. Fan, "All-angle negative refraction for surface plasmon waves using a metal-dielectric-metal structure (vol 96, pg 073907, 2006)," Phys. Rev. Lett. **96**, 073907 (2006).
4. H. Lezec, J. Dionne, and H. Atwater, "Negative refraction at visible frequencies," Science **316**, 430–432 (2007).
5. M. Dennis, N. Zheludev, and F. Garcia de Abajo, "The plasmon Talbot effect," Opt. Express **15**, 9692–9700 (2007).
6. A. Maradudin and T. Leskova, "The Talbot effect for a surface plasmon polariton," New J. Phys. **11**, 033004 (2009).
7. A. Tredicucci, C. Gmachl, F. Capasso, A. L. Hutchinson, D. L. Sivco, and A. Y. Cho, "Single-mode surface-plasmon laser," Appl. Phys. Lett. **76**, 2164–2166 (2000).
8. B. Baumeier, T. A. Leskova, and A. A. Maradudin, "Cloaking from surface plasmon polaritons by a circular array of point scatterers," Phys. Rev. Lett. **103**, 246803 (2009).
9. Y. Liu, T. Zentgraf, G. Bartal, and X. Zhang, "Transformational plasmon optics," Nano Lett. **10**, 1991–1997 (2010).
10. P. A. Huidobro, M. L. Nesterov, L. Martín-Moreno, and F. J. García-Vidal, "Transformation optics for plasmonics," Nano Lett. **10**, 1985–1990 (2010).

#147619 - $15.00 USD Received 24 May 2011; revised 21 Jun 2011; accepted 28 Jun 2011; published 28 Jul 2011

11. J. Renger, M. Kadic, G. Dupont, S. Acimovic, S. Guenneau, and R. Quidant, “Hidden progress: broadband plasmonic invisibility,” Opt. Express **18**, 15757–15768 (2010).
12. R. Zia and M. L. Brongersma, “Surface plasmon polariton analogue to young’s double-slit experiment,” Nat. Nanotechnol. **2**, 426–429 (2007).
13. A. A. Maradudin, “The impedance boundary condition at a two-dimensional rough metal surface,” Optics Commun. **116**, 452 – 467 (1995).
14. K. Atkinson, “The numerical solution of Fredholm integral equations of the second kind with singular kernels,” Numerische Mathematik **19**, 248–259 (1972).
15. F. Huerkamp, T. A. Leskova and A. A. Maradudin, “Surface plasmon polariton analogues of volume electromagnetic wave effects,” Proc. SPIE **7467**, 74670H (2009).
16. Y. A. Nikitin, G. Brucoli, F. J. García-Vidal, and L. Martín-Moreno, “Scattering of surface plasmon polaritons by impedance barriers: Dependence on angle of incidence,” Phys. Rev. B **77**, 195441 (2008).

When an electromagnetic beam of finite cross section is incident from an optically more dense medium on its planar interface with an optically less dense medium, and the polar angle of incidence is greater than the critical angle for total internal reflection, the reflected beam undergoes a lateral displacement along the interface, as if it has been reflected from a plane in the optically less dense medium parallel to the physical interface. This effect was first observed by Goos and Hänchen [1], who measured a displacement $D = 1.495\lambda \pm 0.261\lambda$ for a beam reflected from a silver coated glass-air interface at an angle of incidence $\theta_0 = 44.1^\circ$. This *Goos-Hänchen effect* was explained soon after by Artmann [2], who related it to the phase $\varphi(\theta_0)$ of the amplitude of the reflected beam by

$$D(\theta_0) = -\frac{\lambda}{2\pi}\frac{1}{k_\parallel \cos\theta_0}\left.\frac{d\varphi(\theta)}{d\theta}\right|_{\theta=\theta_0}. \tag{1}$$

In recent years analogues of optical effects originally associated with volume electromagnetic waves have begun to be studied both theoretically and experimentally in the context of surface plasmon polaritons (SPP). These include, *e.g.* negative refraction [3, 4], the Talbot effect [5, 6], lasing [7], cloaking [8, 9, 10, 11] and Young’s double-slit experiment [12]. The interest in such effects is due to a desire to discover new properties of these surface electromagnetic waves and to the possibility of basing novel nanoscale devices on them.

With these motivations, in this paper we study the analogue of the Goos-Hänchen effect for SPP by investigating the system sketched in Fig. 1 in which a SPP propagating on the surface of a metal whose dielectric function is $\varepsilon_1(\omega)$ is incident on a planar interface with an optically less dense metal whose dielectric function is $\varepsilon_2(\omega)$ ($|\varepsilon_2(\omega)| \gg |\varepsilon_1(\omega)|$). We consider the two cases in which the second metal is either infinitely long (single interface) or of finite length L (double interface). The electromagnetic field of the SPP is determined by use of an impedance boundary

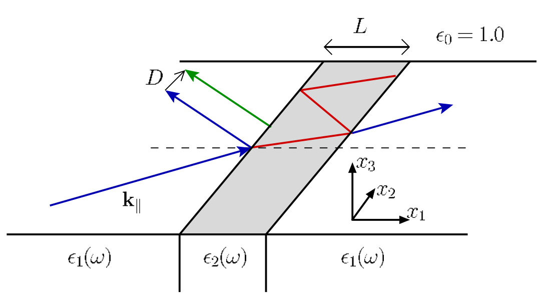

Fig. 1. Scattering geometry of the double interface system. The blue (gray) vectors are the beam reflected from the first interface, the red (black) vectors are the beams reflected from the second interface, and the green (light gray) vectors are the actual reflected beams.

#147619 - $15.00 USD Received 24 May 2011; revised 21 Jun 2011; accepted 28 Jun 2011; published 28 Jul 2011

condition [13] on the surface $x_3 = 0$. Scattering amplitudes $A_i(\mathbf{p}_\parallel)$ for p- and s-polarized fields ($i = p,s$) can be obtained from the solution of a pair of coupled integral equations

$$A_i(\mathbf{p}_\parallel) + \zeta(\omega) \sum_{j=p,s} \int \tilde{S}(\mathbf{p}_\parallel - \mathbf{q}_\parallel) \frac{M_{i,j}(\mathbf{p}_\parallel|\mathbf{q}_\parallel)}{d_j(q_\parallel)} A_j(\mathbf{q}_\parallel) \frac{d^2 q_\parallel}{(2\pi)^2} = -\zeta(\omega)\tilde{S}(\mathbf{p}_\parallel - \mathbf{k}_\parallel) M_{i,p}(\mathbf{p}_\parallel|\mathbf{k}_\parallel). \quad (2)$$

Here, $\zeta(\omega) = \frac{\omega}{c}(\kappa_2(\omega) - \kappa_1(\omega))$ with $\kappa_j(\omega) = i/\sqrt{-\varepsilon_j(\omega)}$ and the terms $M_{i,j}(\mathbf{p}_\parallel|\mathbf{q}_\parallel)$ are given by

$$\begin{aligned} M_{p,p}(\mathbf{p}_\parallel|\mathbf{q}_\parallel) &= -M_{s,s}(\mathbf{p}_\parallel|\mathbf{q}_\parallel) = i\hat{\mathbf{p}}_\parallel \cdot \hat{\mathbf{q}}_\parallel \\ M_{p,s}(\mathbf{p}_\parallel|\mathbf{q}_\parallel) &= -M_{s,p}(\mathbf{p}_\parallel|\mathbf{q}_\parallel) = (\hat{\mathbf{p}}_\parallel \times \hat{\mathbf{q}}_\parallel)_3. \end{aligned} \quad (3)$$

$d_p(q_\parallel) = \beta_0(q_\parallel) + i\frac{\omega}{c}\kappa_1(\omega)$ and $d_s(q_\parallel) = \beta_0^{-1}(q_\parallel) - i\kappa_1(\omega)\frac{c}{\omega}$ denote the dispersion relations for p- and s-polarization, where $\beta_0(q_\parallel) = \sqrt{q_\parallel^2 - \frac{\omega^2}{c^2}}$ with $\mathrm{Re}\,\beta_0(q_\parallel) > 0$ and $\mathrm{Im}\,\beta_0(q_\parallel) < 0$. $\tilde{S}(\mathbf{Q}_\parallel = \mathbf{p}_\parallel - \mathbf{q}_\parallel)$ is the Fourier transformed of the surface profile function

$$\tilde{S}(\mathbf{Q}_\parallel) = \int_{\mathbb{R}^2} S(\mathbf{x}_\parallel) e^{-i\mathbf{Q}_\parallel \cdot \mathbf{x}_\parallel} d^2 x_\parallel = 2\pi\,\delta(Q_2) f(Q_1), \quad (4)$$

where

$$f^{\mathrm{I}}(Q_1) = \frac{1}{i(Q_1 - i\eta)}, \; f^{\mathrm{II}}(Q_1) = \frac{L\,\mathrm{sinc}(Q_1)}{2\exp(\frac{iQ_1 L}{2})} \quad (5)$$

for the single and double interface, respectively. Due to the translational invariance of the system in the x_2-direction $A_{p,s}(\mathbf{q}_\parallel)$ have the general form

$$A_{p,s}(\mathbf{q}_\parallel) = 2\pi\,\delta(q_2 - k_2)\,a_{p,s}(q_1). \quad (6)$$

Substituting Eq. (6) into Eq. (2) leads to a pair of effective one-dimensional integral equations

$$a_i(p_1) + \zeta(\omega) \sum_{j=p,s} \int_{-\infty}^{\infty} M_{i,j}(\bar{\mathbf{p}}_\parallel|\bar{\mathbf{q}}_\parallel) f(p_1 - q_1) \frac{a_j(q_1)}{d_j(\bar{q}_\parallel)} \frac{dq_1}{2\pi} = -\zeta(\omega) M_{i,p}(\bar{\mathbf{p}}_\parallel|\mathbf{k}_\parallel) f(p_1 - k_1), \quad (7)$$

in which we define $\bar{\mathbf{p}}_\parallel = (p_1, k_2)$ and $\bar{\mathbf{q}}_\parallel = (q_1, k_2)$. Equations (7) are solved numerically using the Nystrom method [14]. The infinite range of integration is replaced by a finite interval $[-q_\infty, q_\infty]$. The resulting integrals over q_1 were converted to sums using a N-point extended midpoint method. p_1 was given the values of the abscissas used in the evaluation of the integrals and a square $2N \times 2N$ supermatrix equation with $N = 18001$ for $a_{p,s}(p_1)$ is solved by a standard linear equation solver. The convergence of the solution was monitored by increasing q_∞ and N systematically until the solution did not change upon further increases of these parameters. A lateral displacement of the incident SPP beam is identifiable in the far field region by the intensity distribution of the scattered electromagnetic field of the propagating p-polarized SPP mode with wave number $k_\parallel$. For an incident plane wave, the scattered field is given by

$$\mathbf{E}^{\mathrm{sc}}(\mathbf{x}|\omega) = \int \frac{\hat{\mathbf{e}}_p(q_\parallel) A_p(\mathbf{q}_\parallel)}{\beta_0(q_\parallel) + i\frac{\omega}{c}\kappa_1(\omega)} e^{i\mathbf{q}_\parallel \mathbf{x}_\parallel - \beta_0(q_\parallel)x_3} \frac{d^2 q_\parallel}{(2\pi)^2} \quad (8)$$

#147619 - $15.00 USD Received 24 May 2011; revised 21 Jun 2011; accepted 28 Jun 2011; published 28 Jul 2011

where $\hat{\mathbf{e}}_p(\mathbf{q}_{\|}) = \frac{c}{\omega}\left\{i\hat{\mathbf{q}}_{\|}\beta_0(q_{\|}) - \hat{\mathbf{x}}_3 q_{\|}\right\}$ is the polarization vector for p-polarized SPP. The contribution to this field in the region $x_1 < 0$ from the reflected surface plasmon polariton is given by the residue of the integrand at the simple pole it has at $q_1 = -k_1(\omega) = -\cos(\theta)k_{\|}(\omega)$. With the assumption that $\varepsilon_1(\omega)$ has an infinitesimal positive imaginary part, this pole lies in the lower half of the complex q_1 plane. It can be shown that $a_p(q_1)$ has no pole in this region. On evaluating the residue at this pole we obtain for the electric field of the reflected SPP in the region $x_1 < 0$, $x_3 > 0$

$$\mathbf{E}^{\mathrm{ref}}(\mathbf{x}|\omega) = r(-k_1)\,\frac{c}{\omega}\hat{\mathbf{e}}_p(-k_1,k_2)\,e^{-ik_1x_1+ik_2x_2-\beta_0(k_{\|})x_3}, \tag{9}$$

where $r(-k_1) = \frac{\omega}{c}\kappa_1\frac{a_p(-k_1)}{k_1} = R(-k_1)\,e^{i\,\varphi(-k_1)}$ is the reflection amplitude.

In Fig. 2 we present a plot of R as a function of the angle of incidence when a SPP in the form of a plane wave whose wavelength is $\lambda = 632.8$ nm, propagating on a gold surface with $\varepsilon_1(\omega) = -11.8$ at the corresponding frequency, is incident on its planar interface with aluminum ($\varepsilon_2(\omega) = -64.07$). Since the mean free paths of SPP on these two surfaces are $L_1 = 7\,\mu$m and $L_2 = 30\,\mu$m, we expect the effect of ohmic losses on the our results obtained for real-valued $\varepsilon_i(\omega)$ to be small. The angle of incidence is $\theta = 78°$, and the $1/e$ half width of the beam is $w = 20c/\omega$. The critical angle for total internal reflection, given by $\sin\theta_c = [1-1/\varepsilon_1(\omega)]^{\frac{1}{2}}/[1-1/\varepsilon_2(\omega)]^{\frac{1}{2}}$, has the value $\theta_c = 75.4°$ in this case. Note that preliminary, non-converged results were shown unanalyzed as work in progress in Ref. [15].

It is seen from this figure that R is small ($\sim 10^{-4}$) for all angles smaller than θ_c, and equal to unity for angles greater than θ_{c}. R is not a monotonically increasing function of θ, but has a pronounced minimum at the angle of incidence $\theta \approx 45°$. The occurrence of this dip has been explained for a somewhat different SPP scattering problem as the Brewster effect for the incident SPP [16]. The shift of the position of the minimum in Fig. 2 from $\theta = 45°$ is due to a small imaginary part added to $\varepsilon_1(\omega)$. The phase shift $\varphi(\theta)$ at the interface is close to π for angles smaller than $\theta = 45°$, and jumps to nearly 2π at this angle. In the rather narrow interval $[\theta_{\mathrm{c}}, 90°]$ the phase decreases continuously from 2π to π. Because of the derivative of $\varphi(\theta)$ in Artmann's result one can therefore expect a significant lateral displacement of the reflected beam.

To observe the Goos–Hänchen effect we need the intensity distribution of the field of the reflected SPP when the incident SPP has the form of a beam instead of a plane wave. Such a

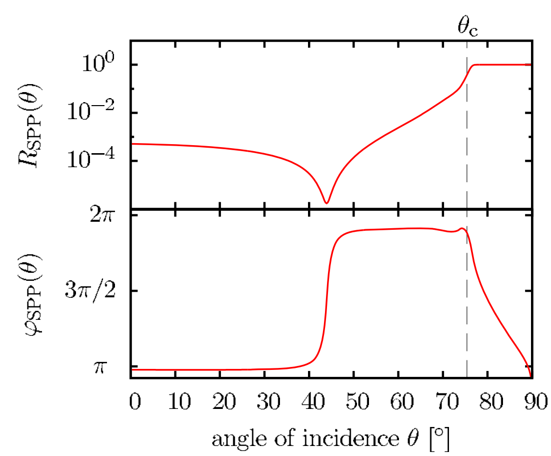

Fig. 2. The modulus of the reflection amplitude R and phase shift φ as functions of the angle of incidence θ for an incident SPP plane wave at the single interface.

#147619 - $15.00 USD Received 24 May 2011; revised 21 Jun 2011; accepted 28 Jun 2011; published 28 Jul 2011

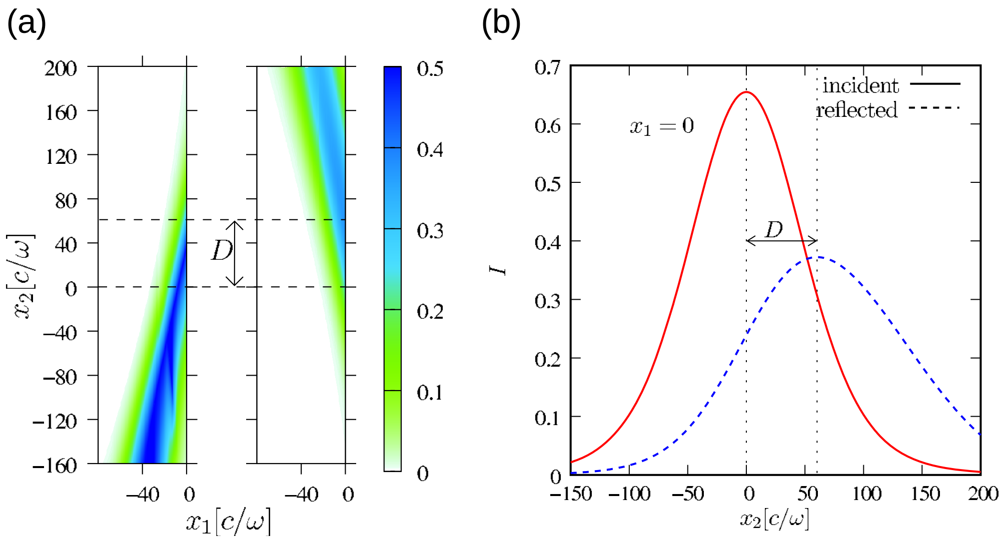

Fig. 3. (a) Color-level plot of the intensity of the incident beam (left), and the reflected beam (right). The angle of incidence is $\theta_0 = 78^\circ$, the beam width is $w = 20\,c/\omega$ and $x_3 = 0.1\,c/\omega$. The maxima of the incident and reflected beam are marked with dashed lines, the displacement is $D = 60.3\,c/\omega = 9.6\lambda$. (b) Plot of the respective intensities along the x_2-direction at the interface ($x_1 = 0$).

field is represented by a superposition of plane waves weighted by a Gaussian function of θ with $1/e$ half width $2/[k_\parallel(\omega)w]$, centered at $\theta = \theta_0$, and normalized to unity, which yields a Gaussian beam of $1/e$ half width w whose angle of incidence is θ_0.

In Fig. 3 we present a color-level plot of the intensity distribution of the incident and reflected SPP beams for the system assumed in obtaining the results plotted in Fig. 2. The positions of the maxima of both beams at the interface ($x_1 = 0$) are marked with a dashed line, showing a displacement of $D = 60.3\,c/\omega = 9.6\lambda$.

In Fig. 4, we compare the results for D as a function of the angle of incidence of the beam θ_0 for different widths of the beam. For a broad beam ($w = 200\,c/\omega$, solid line) we note the existence of a pronounced negative displacement for an angle of incidence close to 45° arising from the jump in the phase shift from π to 2π as in Fig. 2. However, since the reflectivity R is very small (about 10^{-5}) at this angle, it might be difficult to observe this negative displacement experimentally. At θ_c, D increases substantially, and the pronounced peak can be related to the maximum slope of $\varphi(\theta)$ in Fig. 2. The behavior for $\theta_0 \to 90^\circ$ is in agreement with $1/\cos(\theta_0)$ dependence in Artmann's formula. The faint negative D close to θ_c is a result of the use of a small value for $\eta = 0.01$ in $f^{\mathrm{I}}(Q_1)$.

In the case of beams with smaller half widths, Artmann's formula no longer holds, resulting in noticeable differences in the dependence of D on the angle of incidence: the smaller the width, the fewer the structures in $D(\theta_0)$, *e.g.* as in Fig. 4 for beams with $w = 30\,c/\omega$ (dashed line) or $w = 10\,c/\omega$ (dotted line). For instance, the negative displacement at $\theta_0 = 45^\circ$ becomes less pronounced and the feature in the curve smears out. Similar observations can be made for the structures close to the critical angle for total internal reflection. In particular, D remains finite when $\theta_0 \to 90^\circ$.

At a double-interface with $L = 20\,c/\omega$ the phase of a reflected SPP plane wave (see inset of Fig. 5) is identical to the one at the single interface in the interval $[\theta_c, 90^\circ]$ since the wave is totally reflected at the first interface. The major difference is the oscillating behavior at smaller

#147619 - $15.00 USD Received 24 May 2011; revised 21 Jun 2011; accepted 28 Jun 2011; published 28 Jul 2011

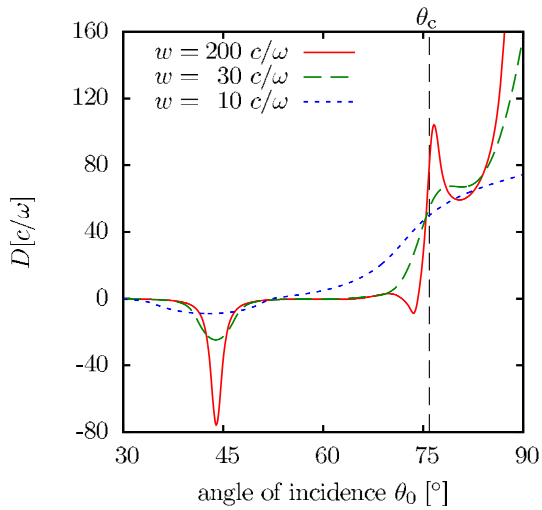

Fig. 4. Calculated lateral displacement D for different beam widths (200, 30, and 10 c/ω) as a function of the angle of incidence of the beam θ_0.

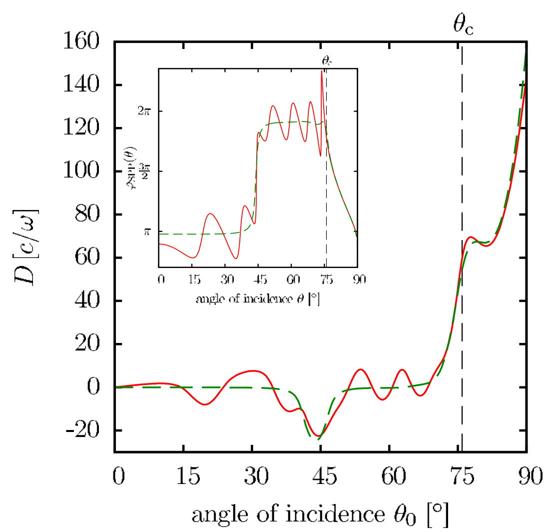

Fig. 5. Lateral displacement as a function of angle of incidence θ_0 at a double interface with $L = 20\,c/\omega$ (solid line) compared to the result for a single interface (dashed line). The width of the SPP beam is $w = 30\,c/\omega$. The inset shows the phase of a reflected SPP plane wave as a function of θ.

angles, which is due to multiple scattering at the two interfaces leading to destructive or constructive interference at different angles as in a Fabry-Pérot interferometer. These oscillations also appear in $D(\theta_0)$ shown in Fig. 5 and decay with larger L.

The absolute values for the lateral displacements of SPP beams of up to 25λ are about one order of magnitude larger than the corresponding results for volume waves [1]. This can be rationalized by the larger critical angle and the concomitantly steeper decrease of the phase in the interval $[\theta_c, 90°]$ in the case of SPP. The values are also sensitive to changes in the dielectric functions. Figure 6 shows the change in D upon variation of either $\varepsilon_1(\omega)$ or $\varepsilon_2(\omega)$ while the

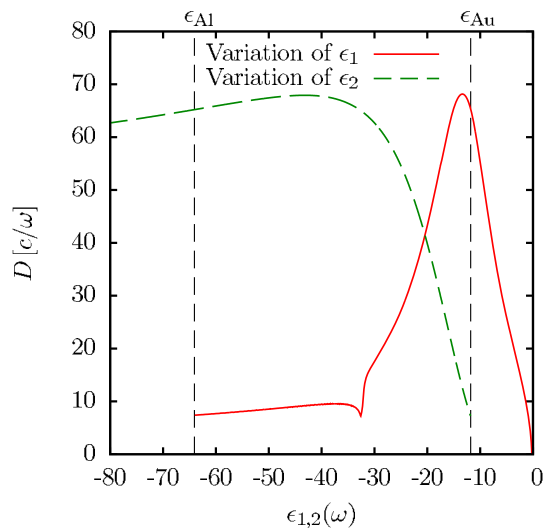

Fig. 6. Change of D upon variation of the dielectric functions of the two metals at an angle of incidence of $\theta_0 = 80^\circ$.

other one is fixed. This results were obtaind by the use of Artmann's formula (1). In particular, the strong dependence of the calculated lateral displacement on the value of $\varepsilon_1(\omega)$, i.e. the dielectric function of the gold surface, indicates that small modifications of the latter may be resolved. Adsorption of molecules changes the dielectric environment of surfaces. Experimental measurements of the Goos-Hänchen effect for SPP for $\theta_0 > \theta_c$, i.e., at grazing incidence, depending on molecular coverage may prove useful in sensing this change and thereby allowing drawing conclusions on adsorption or desorption processes, complementing techniques such as surface plasmon resonance spectroscopy.

In summary, we have demonstrated in this paper the existence of the analogue of the Goos-Hänchen effect for SPPs at a gold-aluminum interface. Due to the large critical angle of $\theta_c \simeq 75^\circ$ for total internal reflection of the SPP, lateral displacements of several times the wavelength of the incident beam occur. The sensitivity of the displacement to changes of the surface optical properties may be exploited to measure, for instance, the modification of the dielectric environment of the metal upon molecular adsorption.

Acknowledgments

BB acknowledges the MMM Initiative of the Max Planck Society. We thank D. Andrienko for a critical reading of the manuscript. FH is grateful to C. Sommer for helpful discussions. TAL and AAM acknowledge support from AFRL contract FA9453-08-C-0230.

#147619 - $15.00 USD Received 24 May 2011; revised 21 Jun 2011; accepted 28 Jun 2011; published 28 Jul 2011